QUARTERLY JOURNAL OF THE ROYAL METEOROLOGICAL SOCIETY

Q. J. R. Meteorol. Soc. **00**: 1–**??** (2007)

Published online in Wiley InterScience

(www.interscience.wiley.com) DOI: 10.1002/qj.000

Propagation, reflection and transmission of precipitation fronts in the tropical atmosphere.

Olivier Pauluis [a]*, Dargan M. W. Frierson [b], Andrew J. Majda [a]

[a] *Courant Institute of Mathematical Sciences, New York University.*

[b] *University of Washington*

KEY WORDS Moist convection, quasi-equilibrium, atmospheric dynamics

Received 18 May 2007; Revised ; Accepted

Abstract

The behavior of the interface between the precipitating and non-precipitating regions is analyzed in an idealized model for the large scale atmospheric circulation. This model uses a quasi-equilibrium relaxation closure in which convection acts to removed the convective instability. It is shown that in the strict quasi-equilibrium limit, i.e. for instantaneous convective adjustment, the boundary between the dry and moist regions can exhibit a discontinuity in the precipitation rate and vertical velocity. This interface, referred here to as a precipitation front, behaves as a propagating shock. Three distinct precipitation fronts can be obtained: drying front, slow moistening front and fast moistening front. The front velocity is distinct from the propagation speed of dry and moist disturbances and must be determined by solving a Riemman problem. Stationary precipitation fronts are also found in steady solutions for idealized Walker circulations in both one and two dimensions. Dry gravity waves and coupled convective-gravity waves are partially

*Correspondence to: Courant Institute of Mathematical Sciences, 251 Mercer street, New York, NY 10012, USA. E-mail: pauluis@cims.nyu.edu.

transmitted and partially reflected when they encounter a precipitation front. Similarly, it is also shown that advection of a water vapor perturbation into a precipitation front generates propagating waves on both sides of the front. For small perturbations, the reflection and transmission coefficients can be determined analytically. For large perturbations, the interaction with the precipitation front is highly nonlinear, and can result in a change in the direction of propagation of the front.

The theory for precipitation fronts discussed here can be viewed as an extension of the Strict Quasi-Equilibrium (SQE) theory for the tropical atmosphere. This theory makes it possible to solve the SQE equations when deep convection is inactive in some portion of the atmosphere, and capture the fundamental non-linearity associated with the onset of precipitation in the SQE framework.

1. Introduction

The interaction between convection and the large-scale circulation is one of the central problems for our understanding of the tropical atmosphere. It is a key element in a wide variety of phenomena, ranging from the Hadley circulation (Satoh 1994; Pauluis 2004), Walker circulation (Bretherton and Sobel 2002), intraseasonal variability (MJO), hurricanes (Emanuel 1986), or equatorial waves (Wheeler and Kiladis 1999). At the core of the interactions lies two fundamental properties of moist air. First, as a parcel of moist air ascends, its temperature decreases because of its adiabatic expansion. After a sufficient drop in temperature, the parcel becomes saturated and water vapor condenses. Hence, any sustained ascending motion in the tropical atmosphere is associated with clouds and precipitation. Second, the condensation of water vapor results in a significant release of latent heat that compensates partially for the adiabatic cooling. This latent heat release modifies the temperature of the atmosphere, which in turn impacts the circulation. The balance between these two feedbacks – the enhancement of precipitation in ascending regions, and the atmospheric response to latent heat release – has profound implications for the dynamics of the tropical regions.

The large scale separation between convective motions, which take place on horizontal scales of 10km or less, and the synoptic and planetary scales (1,000 km to 10,000 km) has prevented until recently explicit numerical simulations that would resolve both the convective and planetary scales. In General Circulation Models (GCM's), which are designed to study the planetary and synoptic scale circulation, the horizontal resolution is of the order of 100 km, and is insufficient to adequately resolve convective motions. Instead, GCM's rely on cumulus parameterizations that determine the behavior of convective systems based on semi-empirical closure assumptions.

One of the most successful convective closures is the quasi-equilibrium theory originally proposed by Arakawa and Schubert (1974) and is at the core of other representations of convection such as that of Betts and Miller (Betts 1986; Betts and Miller 1986), or Emanuel (1991). The quasi-equilibrium theory postulates that convective motions act to eliminate convective instability over a convective adjustment time-scale of a few hours. As a result, a convective region is in a state of quasi-equilibrium between the destabilizing effects of the large-scale circulation and external heat sources and the stabilization by convective motions. As the convective adjustment time-scale is short in comparison to the time-scale associated with synoptic or planetary circulation, the amount of convective instability, quantified in terms of the cloud work function (Arakawa and Schubert 1974) or Convective Available Potential Energy (Xu and Emanuel 1989) remains small in convectively active regions.

The quasi-equilibrium theory predicts the existence of coupled convective-gravity waves resulting from the interaction of convection and large-scale circulation (Neelin et al. 1987; Emanuel 1987; Emanuel et al. 1994, ENB herfater). In the quasi-equilibrium framework, convection is more intense during periods of large scale ascent, so that latent heat release due to condensation compensates partially for the adiabatic cooling. As a result of this correlation between latent heat release and vertical ascent, the propagation speed of a disturbance is reduced in comparison to what it would be in the absence of condensation. Wheeler and Kiladis (1999) have recently used satellite observations to identify such coupled-convective gravity modes, as well as their faster uncoupled counterparts. They estimate that coupled convective gravity waves propagate horizontally at a speed of about 15 $m\ s^{-1}$, which is about three times slower than a dry wave with the same depth.

One of the key parameters in quasi-equilibrium closures is the convective adjustment time, i.e. the time it takes for convection to remove convective instability. Various studies argue that this time should be between 2 and 24 hours (Betts 1986; Bretherton et al. 2004)). Given that this time scale is much shorter than the time scale of the planetary scale circulation, ENB have proposed the Strict Quasi-Equilibrium (SQE) as the limit of the quasi-equilibrium theory for infinitely short convective adjustment time. In SQE, the atmospheric is instantaneously relaxed toward a moist adiabatic density profile in convective regions, and this eliminates the need for a described description of the behavior of individual clouds. As such, SQE offers a very elegant simplifying assumption for theoretical investigations of the interaction of convection and the planetary scale.

The SQE framework as presented in ENB has an important limitation: it can only be applied for an atmosphere where there is precipitation everywhere. The main question here is not how to describe the behavior of the atmosphere within the dry (non-precipitating) and the moist (precipitating) regions, but rather how to determine the evolution of the

interface between these two regions. This problem arises directly from the physical requirement that the precipitation rate P can only be positive:

$$P \geq 0. \tag{1}$$

This constraint imposes a strong nonlinearity on the flow, as any solution of the equations of motion which produces a given precipitation rate $P > 0$, the reverse circulation would require a negative precipitation rate and is thus is not realizable. The primary goal of this paper is to describe the behavior of the interface between the dry and moist regions and to analyze the nonlinearity associated with the onset of precipitation.

Frierson et al. (2004) demonstrates the existence of precipitation fronts in an idealized model of the tropical atmosphere. A simplifed discussion of the mathematical framework of Frierson et al. (2004) is presented in section 2. The model equations are similar to that of the Quasi-equilibrium Tropical Circulation model (QTCM Neelin and Zeng (2000)), with a quasi-equilibrium closure for the precipitation rate. It is shown the quasi-equilibrium formulation for the precipitation is dissipative. In the limit of infinitely short adjustment time, the dissipation is concentrated at the interface between the dry and moist regions. This interface exhibits a discontinuity in precipitation and vertical velocity, and in the horizontal temperature and humidity gradients. These precipitation fronts behave as dynamical shocks, moving at a velocity that differs from the dry and moist propagation speeds. Three types of fronts are identified: the drying fronts, the slow moistening fronts and the fast moistening fronts.

In section 3, the theory for precipitation fronts is applied to obtained stationary solutions for an idealized Walker circulation. In the SQE limit, one-dimensional Walker circulations can exhibit a discontinuity similar of the precipitation rate at the edge of the precipitation region. The presence of the discontinuity depend critically on both the position of the precipitation region relatively to the wind, and on the intensity of the wind itself. For wind velocity that are smaller than the propagation speed of moist wave, the precipitation front is located on the upwind side of the precipitation regions. The results for the one-dimensional Walker cell are also generalized to two-dimensional Walker circulations on a beta-plane.

The fourth section shows the behavior of precipitation fronts can be determined by solving a Riemann problem. In the dry regions, the SQE equations are described by three Riemann invariants, two of them corresponding to the invariants for the shallow water equations, and a third one corresponding to a moisture trace. In the moist regions, two invariants are sufficient to describe the state of the atmosphere. Each type of precipitation front intercepts three different characteristics, while only two characteristics are radiating away from the front. It is shown that the front velocity and the Riemann invariants on these outgoing characteristics are uniquely determined by the invariants on the incident

characteristics. It is also shown that precipitation fronts are associated with a nonlinear transmission and reflection of a signal incident on the fronts. In the case of a small perturbation, linear reflection and transmission coefficients can be determined analytically. These calculations indicates that the precipitation fronts can be associated both with over-reflection, and amplification of the transmitted signal. It is also shown that the encounter of a precipitation front and a humidity perturbation will generate gravity waves on both sides of the fronts.

These results are summarized in the last section. It is argued that the combination of the SQE limit and the theory for precipitation fronts offers one of the simplest frameworks to study the large-scale circulation in the tropical atmosphere. The theory for precipitation fronts outlined here describes the behavior of the interface between dry and moist regions, both in terms of the displacement of the interface, and in terms of the transfer of signals between the dry and moist regions. The precipitation front theory leads to an interesting prediction that incident waves should be partially reflected and partially transmitted when encountering the interface between the dry and moist regions.

2. Precipitation Fronts

2a. *Model equations*

The model used here is based on a Galerkin truncation of the equations of motion into a finite set of vertical modes. For simplicity, only the first two modes are reatined, as in the QTCM. The zonal wind is given as the sum of the barotropic wind $\overline{\mathbf{U}}$ and first baroclinic mode $\mathbf{U_1}$: $\mathbf{U}(x,y,z) = \overline{\mathbf{U}}(x,y) + \mathbf{U_1}(x,y)\Psi_U(z)$, with $\Psi_U(z) = cos(z)$ the structure function for the zonal wind (z is a nondimensional depth that ranges from 0 at the surface to 1 at the tropopause). The temperature and humidity are given by $T(x,y,z) = \overline{T}(z) + T_1(x,y)\Psi_T(z)$ and $\overline{Q}(z) + Q_1(x,y)\Psi_Q(z)$, where $\overline{T}(z)$ and $\overline{Q}(z)$ are horizontally uniform temperature and humidity reference profiles, and $\Psi_T(z) = sin(z)$ and $\Psi_Q(z)$ are the structure function for temperature and humidity. We ignore diabatic sources such as evaporation and radiative cooling in this section for simplicity, but add these in Section 3 in our examination of the steady Walker cell. The equations of motion on an equatorial β-plane, after Frierson et al. (2004), are

$$\partial_t \overline{\mathbf{U}} + \overline{\mathbf{U}} \cdot \nabla \overline{\mathbf{U}} + \mathbf{U_1} \cdot \nabla \mathbf{U_1} = -y\mathbf{k} \times \overline{\mathbf{U}} - \nabla \overline{\Phi} \tag{2a}$$

$$\partial_t \mathbf{U_1} + \overline{\mathbf{U}} \cdot \nabla \mathbf{U_1} + \mathbf{U_1} \cdot \nabla \overline{\mathbf{U}} = -y\mathbf{k} \times \mathbf{U_1} + \nabla T_1 \tag{2b}$$

$$\partial_t T_1 + \overline{\mathbf{U}} \cdot \nabla T_1 = c_d^2 \nabla \cdot \mathbf{U_1} + P \tag{2c}$$

$$\partial_t Q_1 + \overline{\mathbf{U}} \cdot \nabla Q_1 = -c_d^2 \Delta \overline{Q} \nabla \cdot \mathbf{U_1} - P \tag{2d}$$

$$\nabla \cdot \overline{\mathbf{U}} = 0 \tag{2e}$$

In the absence of precipitation and with no barotropic wind, the equations for baroclinic wind $\mathbf{U_1}$ and temperature reduce to the shallow water equations with characteristic speed c_d, This dry propagation speed is given by $c_d^2 = \pi^{-1} H C_p \partial_z \overline{T} + gH$, with H the depth of the atmosphere, and C_p the heat capacity at constant pressure. Typical values for the tropical atmosphere yield a propagation speed of 40-50 ms^{-1}. The moisture stratification $\Delta \overline{Q}$ is a function of the reference humidity profile $\overline{Q}$ and structure function. A complete derivation of these equations is available in Frierson et al. (2004), which is itself adapted from the procedure used in the QTCM (Neelin and Zeng 2000). Notice also that a similar set of equations can be derived for a two-layer system such as in Lapeyre and Held (2004). Note that while the humidity is primarily concentrated in the lower troposphere, the humidity advection in our model is done solely by the barotropic wind. This results from the use of a uniform structure function in height for the humidity. In contrast, the QTCM which includes a baroclinic advection term in the moisture equation. The potential consequences of such baroclinic moisture advection for the dynamic of the precipitation fronts are discussed in the final section.

This system of equations is incomplete until we specify the precipitation rate. We consider here a simple representation of deep convection in which precipitation relaxes the humidity perturbation to a reference value (in non-dimensional units) in regions where deep convection is active. In regions where there is convective inhibition, i.e., where the perturbation humidity is smaller than the critical value, the precipitation vanishes. This yields

$$\begin{aligned} P &= \frac{Q_1 - Q_*}{\tau} \text{ for } Q_1 > Q_* \\ &= 0 \text{ for } Q_1 \leq Q_*. \end{aligned} \tag{3}$$

Here, τ is the relaxation time, and Q_* is the critical humidity at which convection is initiated. The critical humidity can be chosen to be a function of temperature $Q_* = Q_s + \alpha T_1$, and equation can be viewed as relating the amount of precipitation to the amount of Convective Available Potential Energy (APE) in the column. It is shown in Frierson

et al. (2004) that, if a new humidity variable is defined by $Q_1' = Q_1 - Q_s - \alpha T_1$, one obtains a new set of equations is mathematically equivalent to the case $Q_* = 0$, so only this case is discussed hereafter. [†]

In the limit of vanishing τ, precipitation instantaneously relaxes the water content to its saturation value $Q_* = 0$ in the moist region, with the precipitation to be given by

$$\begin{aligned} P &= -c_d^2 \Delta\overline{Q} \nabla \cdot \mathbf{U_1} \text{ for } Q_1 = 0 \text{ and } \nabla \cdot \mathbf{U_1} < 0 \\ P &= 0 \text{ otherwise.} \end{aligned} \tag{4}$$

In this case, the temperature equation (2c) in the moist regions can be written as

$$\partial_t T_1 + \overline{\mathbf{U}} \cdot \nabla T_1 = (1 - \Delta\overline{Q}) c_d^2 \nabla \cdot \mathbf{U_1}. \tag{5}$$

In the SQE limit, the governing equation in the moist regions (2b) and (5) behaves as the shallow water equations with a moist propagation speed c_m that is smaller than the propagation speed in the dry region:

$$c_m = (1 - \Delta\overline{Q})^{1/2} c_d. \tag{6}$$

In our simplified model, $\Delta\overline{Q}$ is the ratio of the latent heat stratification to the dry static energy stratification. Yu et al. (1998) have shown that in the tropics, these two quantities are almost equal, with $\Delta\overline{Q} \approx 0.9$. This implies that the moist speed is approximately $c_m \approx 0.3 c_d \approx 15 m s^{-1}$.

In the absence of barotropic flow ($\overline{\mathbf{U}} = 0$), the equations (2b-2d) reduce to the linear shallow water equations, with different propagation speeds in the dry and moist regions. The problem however remains nonlinear because of the transition from precipitating $P > 0$ to non-precipitating $P = 0$. The nonlinearity is associated with the behavior of the interface between dry and moist regions, and affects both how the interface moves, and how a signal propagates across it. Before studying the interface in section 2d, one must first ensure that the SQE limit is at least mathematically consistent when dry and moist regions are present.

2b. *Dissipation in quasi-equilibrium*

In this section, we show that the solutions of (2a-2a) are well-behaved in the SQE limit of infinitely short convective adjustment. Well-behaved here means that solutions are bounded and obey certain smoothness properties. From a physical point of view, a quantity that can be interpreted as a moist version of the available potential energy is found to be decreasing with time, implying that the SQE system is dissipative.

[†]From a physical point of view, the rescaled variable $Q_1' = Q_1 - Q_s - \alpha T_1$ measures of the instability in the column, and the humidity variable in the case $Q_* = 0$ should be interpreted as an ersatz for CAPE.

For simplicity, only an atmosphere with no barotropic wind $\overline{\mathbf{U}} = 0$ is considered here. An equation for the sum of the available potential energy and kinetic energy can be obtained by multiplying (2a) by $c_d^2 \mathbf{U_1}$ and (2c) by T_1 and adding them together:

$$\partial_t \left(\frac{c_d^2 |\mathbf{U_1}|^2}{2} + \frac{T_1^2}{2} \right) = \nabla \cdot (c_d^2 \mathbf{U_1} T_1) + P T_1. \tag{7}$$

In the absence of precipitation ($P = 0$), the right-hand side is the divergence of a flux, and equation (7) corresponds to the global conservation of the sum of the available potential energy and kinetic energy in the shallow water equations. When precipitation is present however, it can act as a source or a sink of available potential energy depending on whether it is positively or negatively correlated with temperature. Hence, the sum of available and kinetic energy is not necessary conserved, as would have been the case in the absence of precipitation.

One way around this problem is to add an additional component to the energy equation to account for the fluctuations of moisture. First, a saturation temperature is defined by $T_{\mathrm{w}} = T_1 + \frac{Q_1}{\Delta \overline{Q}}$. Its tendency is obtained by combining equations (2c) and (2d) :

$$\partial_t T_{\mathrm{w}} = \partial_t \left(T_1 + \frac{Q_1}{\Delta \overline{Q}} \right) = -\frac{1 - \Delta \overline{Q}}{\Delta \overline{Q}} P \tag{8}$$

The quantity $T_{\mathrm{w}} = T_1 + \frac{Q_1}{\Delta \overline{Q}}$ can be thought of as the temperature that the atmosphere column would have if it were brought to saturation ($Q_1 = 0$) by imposing the necessary vertical motion in the column. Note that this saturation temperature is only affected by precipitation which always reduces it.

We can now define a quantity S as

$$\begin{aligned} S &= \frac{c_d^2 |\mathbf{U_1}|^2}{2} + \frac{T_1^2}{2} + \frac{\Delta \overline{Q}}{1 - \Delta \overline{Q}} \frac{T_{\mathrm{w}}^2}{2} \\ &= \frac{c_d^2 |\mathbf{U_1}|^2}{2} + \frac{T_1^2}{2} + \frac{(\Delta \overline{Q} T_1 + Q_1)^2}{2 \Delta \overline{Q} (1 - \Delta \overline{Q})}. \end{aligned} \tag{9}$$

The tendency for S is

$$\partial_t S - \nabla \cdot (c_d^2 \mathbf{U_1} T) = -\frac{P Q_1}{\Delta \overline{Q}}. \tag{10}$$

In quasi-equilibrium, the precipitation is correlated with humidity (2a), and the second term on the right hand-side is always negative:

$$\partial_t S - \nabla \cdot (c_d^2 \mathbf{U_1} T) \leq 0. \tag{11}$$

This indicates that the quasi-equilibrium system is a dissipative system. On a closed domain, the integral of S can only decrease. As this integral is a L2 norm, this guarantees that solutions remains bounded for all time. In SQE,

the correlation between P and Q vanishes in the dry and moist regions. It may seem that the system becomes non-dissipative. However, as τ^{-1} becomes infinitely large, there is significant dissipation in a narrow region at the interface between the dry and moist regions.

2c. *Gradient formulation*

Remarkably, the dissipative nature of the SQE system extends to the first order derivative. The equations of motion can be written in terms of the divergence $D_1 = \nabla \cdot \mathbf{U_1}$ and vorticity $\zeta = \nabla \times \mathbf{U_1}$ of the baroclinic wind:

$$\partial_t D_1 = \nabla \cdot \nabla T_1 - u_1 + y\zeta_1 \tag{12a}$$

$$\partial_t \zeta_1 = -v_1 - yD_1 \tag{12b}$$

$$\partial_t \nabla T_1 = c_d^2 \nabla D_1 + \nabla P \tag{12c}$$

$$\partial_t \nabla Q_1 = -c_d^2 \Delta\overline{Q} \nabla D_1 - \nabla P. \tag{12d}$$

Here, u_1 and v_1 are the zonal and meridional components of the baroclinic wind. A quantity S_1 is defined by

$$S_1 = \frac{c_d^2 D_1^2 + c_d^2 \zeta_1^2 + |\nabla T_1|^2}{2} + \frac{|\Delta\overline{Q}\nabla T_1 + \nabla Q_1|^2}{2\Delta\overline{Q}(1-\Delta\overline{Q})}. \tag{13}$$

Its tendency is given by

$$\partial_t S_1 + \nabla \cdot (c_d^2 D \nabla T_1) + \partial_x (c_d^2 (u_1^2 + v_1^2)) + c_d^2 (u_1 \partial_y v_1 - v_1 \partial_y u_1) = -\frac{\nabla P \cdot \nabla Q_1}{\Delta\overline{Q}}. \tag{14}$$

The fourth term on the left-hand side is not a flux, and can potentially lead to a global increase in the integral of S_1. This term can be traced back to variation of planetary vorticity and disappears for $\beta = 0$ or in the absence of rotation. As it is also independent of the convective adjustment time, any growth it might induce would take place on time scales much longer than τ in the SQE limit.

In contrast, as long as the precipitation is a monotonically increasing function of humidity ($\frac{dP}{dQ_1} > 0$), the right-hand side of (14) is always negative:

$$-\frac{\nabla P \cdot \nabla Q_1}{\Delta\overline{Q}} = -\frac{\frac{dP}{dQ}|\nabla Q_1|^2}{\Delta\overline{Q}} < 0. \tag{15}$$

Precipitation acts as a dissipative mechanism that reduces the global integral of S_1.

The fact that precipitation acts as a dissipative mechanisms for the quantities S and S_1 has important implications for the mathematical behavior of the solutions. The global integral of the sum of S and S_1 is a norm for the Sobolev

space H_1 of functions with square integrable first derivatives. Such a space includes continuous functions which are piecewise differentiable, but excludes discontinuous functions. The dissipative nature of S and S_1 guarantees that if one starts with an initial condition belonging to the Sobolev space H_1, it will remain there at all time. In particular, solutions with smooth initial conditions do not develop any discontinuities in U, T, or Q. This also ensures that solutions with discontinuities in their first order derivatives are well-behaved and can be solved in the weak sense.

Higher order derivatives do not exhibit the same dissipative properties. If one constructs an equivalent to S_1 based on the second derivatives, its tendency would include a term in

$$-\partial_{xx}P\partial_{xx}Q = -\frac{dP}{dQ}(\partial_{xx}Q)^2 - \frac{d^2P}{dQ^2}(\partial_x Q)^2\partial_{xx}Q.$$

The second term on the right-hand side can be of either sign, and second order derivatives can grow indefinitely. Furthermore, such growth would occur on the convective timescale. In the SQE limit of infinitely fast adjustment, this corresponds to an instantaneous generation of a discontinuity in the first derivatives of the state variables and in the precipitation rate. These discontinuities, which represent the infinitely sharp interfaces between dry and moist regions which develop in SQE, we call "precipitation fronts."

2d. *Propagation of precipitation fronts*

To develop a theory for the movement of the interfaces between dry and moist regions in the tropics, we consider here the propagation of a precipitation front in a one-dimensional channel, with no rotation or barotropic wind. In this case, the prognostic variables are the vertical velocity $W = -D_1$, and the zonal gradients of temperature $T_x = \partial_x T_1$ and humidity $Q_x = \partial_x Q_1$:

$$\partial_t W = -\partial_x T_x \tag{16a}$$

$$\partial_t T_x = -c_d^2 \partial_x W + \partial_x P \tag{16b}$$

$$\partial_t Q_x = \Delta\overline{Q} c_d^2 \partial_x W - \partial_x P \tag{16c}$$

Discontinuities in W, T_x, or Q_x are handled by using a weak formulation of the equations in which the governing equations (16a - 16c) are integrated across the discontinuity. The fact that such solutions are mathematically well-behaved is guaranteed by the dissipation of the quantities S_0 and S_1 discussed in the previous section. Solutions are assumed to be of the form $(W, T_x, Q_x)(x - st, t)$ with the discontinuity located at $x - st = 0$ and s the displacement speed of the discontinuity. It is assumed here without loss of generality that the moist region is located on the positive side of the front.

For an equation of the form

$$\partial_t \phi = \partial_x F(\phi),$$

integrating across a jump at x = 0 yields

$$-s[\phi] = [F(\phi)]$$

The bracket denotes a difference taken across the interface $[\phi] = \phi_+ - \phi_-$, and the indices $+$ and $-$ refer to the value of the function on the right and left side of the interface. The key assumption here is that the solution ϕ remains square integrable at all time. In the case of the moisture fronts, the dissipation of S and S_1 (equations 10 and 14) guarantees that the solutions are well-defined. Applying this procedure to (16a - 16c) yields:

$$-s[W] = -[T_x] \tag{17a}$$

$$-s[T_x] = -c_d^2[W] + [P] \tag{17b}$$

$$-s[Q_x] = c_d^2 \Delta\overline{Q}[W] - [P]. \tag{17c}$$

This is a system of 3 equations with 9 unknowns. One can also take advantage of the properties of the solutions in the dry and moist regions to obtain additional constraints on the solutions.

In the moist regions, we have three constraints:

$$P_+ \geq 0 \tag{18a}$$

$$Q_{x_+} = 0 \tag{18b}$$

$$P_+ = c_d^2 \Delta\overline{Q} W_+. \tag{18c}$$

The first constraint is the requirement that precipitation be positive at all times. The second arises from the fact that the humidity is equal to the convective threshold. The third equation is obtained by taking $\partial_t Q = 0$ in the moisture equation.

For the dry regions, three constraints can be obtained:

$$P_- = 0 \tag{19a}$$

$$Q_{x-} \geq 0 \tag{19b}$$

$$sQ_{x-} = -\Delta\overline{Q} W_- \tag{19c}$$

The first constraint here is the requirement that here be no precipitation in the dry regions. The second results from the fact that the humidity must be lower than the convective threshold in the dry regions, but is equal to it at the interface with the moist region. The third constraint is the equation for the discontinuity in Q_x in (17c), in which the constraint on P_+ and Q_{x+} have been used.

Using the constraints on P_- and P_+ in equation (17b) yields

$$-s[T_x] = c_d^2 W_- - c_m^2 W_+. \tag{20}$$

An expression for the propagation speed s is then obtained by combining this latter equation with (17a):

$$s^2 = \frac{c_m^2 W_+ - c_d^2 W_-}{W_+ - W_-}. \tag{21}$$

However, not all values of s are realizable due to two requirements: that precipitation be positive in the moist region $P_+ \geq 0$, and that the moisture must be lower than the convective threshold in the dry region ($Q_{x-} \geq 0$). Using these constraints with 21, one finds that three different sets of acceptable solutions can be obtained, leading to the classification of preciptation fronts into three distinct categories: drying fronts, slow moistening fronts and fast moistening fronts.

A drying front occurs when the interface moves into the moist region ($s > 0$). The constraints (19b) and (19c) imply that the vertical velocity on the dry side must be negative, $W_- \leq 0$. It then follows that the displacement speed (21) is between the moist and dry propagation speeds:

$$\text{Drying front} : W_+ > 0,\ W_- < 0,\ c_m < s < c_d. \tag{22}$$

Moistening fronts correspond to the situation where the interface moves into the dry region ($s < 0$). In this case, the constraints (19b) and (19c) indicate that the vertical velocity is positive in the dry region $W_- \geq 0$. Equation (21) can be written as:

$$\frac{W_-}{W_+} = \frac{c_m^2 - s^2}{c_d^2 - s^2} \tag{23}$$

This ratio can be positive only if either $s^2 > c_d^2$ or $s^2 < c_m^2$. The first case corresponds to a front faster than dry waves:

$$\text{Fast moistening front} : W_- > W_+ > 0, s < -c_d. \tag{24}$$

The negative front velocity here indicates a front propagating into the dry regions ($x < 0$). The second corresponds to a slow moistening front with the following characteristics:

$$\text{Slow moistening front} : W_+ > W_- > 0,\ -c_m < s < 0. \tag{25}$$

The numerical experiments presented in Frierson et al. (2004) show that all three types of front are realizable and stable.

3. Stationary Solutions

3a. *One-dimensional Walker Cell*

In the previous section, propagating precipitation fronts are shown to be a solution of the idealized atmospheric model in the strict quasi-equilibrium limit. It is also possible to obtain stationary fronts. Let us first derive a steady solution for a one-dimensional Walker circulation with imposed evaporation E and radiation R. For a steady solution, the equations of motion are

$$-\overline{U}W = \partial_x T \tag{26a}$$

$$\overline{U}\partial_x T = -c_d^2 W + P - R \tag{26b}$$

$$\overline{U}\partial_x Q = c_d^2 \Delta\overline{Q} W - P + E \tag{26c}$$

In this problem, a prescribed barotropic wind $\overline{U}$ is imposed. It is also assumed here that the evaporation and radiation are smooth functions of x. The existence of steady solutions requires that the average radiation balances the average evaporation:

$$\int R dx = \int E dx. \tag{27}$$

In the absence of barotropic wind, $\overline{U} = 0$, equation (26a) implies that the temperature is uniform in a steady state solution $\partial_x T = 0$. Adding (26b) and (26c) together also indicates that the vertical velocity W is as smooth as the radiation and evaporation. Hence, in the absence of barotropic flow, the stationary solution is as smooth as the forcing terms E and R, i.e., there is no stationary precipitation front.

In the presence of a barotropic flow $\overline{U} \neq 0$, steady solutions can exhibit precipitation fronts, even when the radiation and evaporation fields are smooth. A necessary condition for the presence of a steady front is derived from equations (26a-26c). The precipitation rate can be obtained from equations (26a-26b):

$$P = R + (c_d^2 - \overline{U}^2)W. \tag{28}$$

As the precipitation vanishes in the dry region and the radiation is smooth, the precipitation on the moist side of the front P_m is given by

$$P_m = (c_d^2 - \overline{U}^2)(W_m - W_d), \tag{29}$$

where the subscripts d and m refer to values evaluated at the dry and moist side of the boundary between dry and moist regions. Adding (26c) and (28) yields

$$(c_m^2 - \overline{U}^2)W = -\overline{U}\partial_x Q + E - R \tag{30}$$

For smooth radiation and evaporation fields, using the fact that the humidity is uniform in the moist region ($\partial_x Q_m = 0$), we get

$$(c_m^2 - \overline{U}^2)(W_m - W_d) = \overline{U}\partial_x Q_d \tag{31}$$

Eliminating $W_m - W_d$ between (29) and (31) yields

$$P_m = \frac{c_d^2 - \overline{U}^2}{c_m^2 - \overline{U}^2}(\overline{U}\partial_x Q_d) \tag{32}$$

For a given $\overline{U}$, the requirement that the precipitation be positive translates into a constraint on the sign of $\overline{U}\partial_x Q_d$. We refer here to upwind and downwind fronts depending on the position of the dry regions in relation to the frontal discontinuity. For an upwind front, the barotropic wind advects dry air into the frontal region. This situation is characterized by a negative correlation between the barotropic wind and water vapor gradient: $\overline{U}\partial_x Q_d > 0$. For a downwind front, this correlation is negative $\overline{U}\partial_x Q_d < 0$. Equation (32) then yields a necessary condition for the existence of precipitation fronts:

1) Upwind fronts can only exist for $|\overline{U}| \leq c_m$ or $|\overline{U}| > c_d$.

2) Downwind fronts are present for $c_m < |\overline{U}| < c_d$.

Notice that the first condition corresponds to the condition for the existence of a moistening front traveling at the speed $s = -\overline{U}$. Similarly, the second condition corresponds to existence of a drying front moving at the speed $s = -\overline{U}$.

3b. *Analytic solution for 1-D Walker circulation*

Let us consider now a steady Walker solution on a periodic domain for a weak easterly barotropic wind $-c_m < \overline{U} < 0$. In this case, if a precipitation front is present, it should be on the Eastern (upwind) side of the precipitating region, as the precipitation rate must vary smoothly on the Western (downwind) side of the moist region.

In the moist region, the solution of (26a-26c) is given by

$$\partial_x Q = 0 \tag{33a}$$

$$\partial_x T = -\overline{U} W \tag{33b}$$

$$W = \frac{E - R}{c_m^2 - \overline{U}^2} \tag{33c}$$

$$P = \frac{c_d^2 - \overline{U}^2}{c_m^2 - \overline{U}^2} E - \frac{c_d^2 - c_m^2}{c_m^2 - \overline{U}^2} R. \tag{33d}$$

If the precipitation rate (33d) is always positive, then the moist region extends through the entire domain in steady state.

When the precipitation rate given by (33d) is negative in some portion of the domain, there must be a dry (non-precipitating) region. In this region, the solution is given by

$$P = 0 \tag{34a}$$

$$\partial_x T = -\overline{U} W \tag{34b}$$

$$W = \frac{-R}{c_d^2 - \overline{U}^2} \tag{34c}$$

$$\partial_x Q = E - \frac{c_d^2 - \overline{c}_m^2}{c_d^2 - \overline{U}^2} R. \tag{34d}$$

The issue here is to find the location of the interface between the dry and moist regions. Here, we take advantage of the fact that for our choice of the barotropic wind $-c_m < \overline{U} < 0$, only a downwind front can be present. This implies that the precipitation rate must be smooth on the western side of the moist region. The location x_W is chosen as one where the precipitation rate (33d) must vanish:

$$\frac{E(x_W)}{R(x_W)} - \frac{c_d^2 - c_m^2}{c_d^2 - \overline{U}^2} = 0. \tag{35}$$

For x_W to correspond to the western boundary of the precipitation regions, the precipitation rate must increase with x, i.e. $\frac{d}{dx}(\frac{E}{R}) > 0$. If equation (35) has only two roots, the location of the western boundary is uniquely determined. [‡] The moisture field in the dry region can be obtained by integrating (34d) westward:

$$Q(x) = Q_* - \int_x^{x_W} \left(E - \frac{c_d^2 - \overline{c}_m^2}{c_d^2 - \overline{U}^2} R \right) dx \tag{36}$$

[‡]If there are more roots, some roots may not yield a valid solution, but at least one would. In this case, the proper solution would have to be found by trial and error on the different roots.

The location of the Eastern edge of the moist regions corresponds to the point x_E where the atmosphere becomes saturated again, i.e. where $Q(x_E) = 0$ in (36). Once x_E and x_W are found, the vertical velocity field can be determined directly, and the temperature field can be obtained by integrating (33b) and (34b).

Figure 1 shows solutions for a forcing given by

$$R = 1 \tag{37}$$

$$E = 1 + E_0 sin(\frac{2\pi x}{L}). \tag{38}$$

Here, $L = 40,000km$ is the length of the domain. The value of c_d and c_m are $45ms^{-1}$ and $15ms^{-1}$ respectively. The two controlling parameters for this problem are $\overline{\mathbf{U}}$ and E_0. Here, we use a mean wind of $\overline{\mathbf{U}} = -0.1c_d(4.5ms^{-1})$and vary the parameter E_0 from $E_0 = 0.1$, $E_0 = 0.2$, and $E_0 = 0.4$. All solutions exhibit a stationary precipitation front at the upwind side of the precipitation region, with discontinuities in the precipitation and vertical velocity. In contrast, the solution is smooth on the downside side of the precipitation regions.

3c. *Two-dimensional Walker cells*

On an equatorial beta-plane, the general solution would require a complete description of the frontal dynamics in two dimensions, and is beyond the scope of the present paper. Rather, solutions to the two-dimensional Walker circulation problem are derived from 1D solutions, and are shown to exhibit fronts. Consider the equations of motion on an equatorial beta-plane for a steady flow:

$$\overline{U}\partial_x u_1 = \beta y v_1 + \partial_x T \tag{39a}$$

$$\overline{U}\partial_x v_1 = -\beta y u_1 + \partial_y T \tag{39b}$$

$$\overline{U}\partial_x T = c_d^2(\partial_x u + \partial_y v) + P - R \tag{39c}$$

$$\overline{U}\partial_x Q = -\Delta\overline{Q}c_d^2(\partial_x u + \partial_y v) - P + E \tag{39d}$$

Here, we consider only solutions that are decaying away from the equator, with a structure function of the form $\exp(-\alpha y^2)$, with α an arbitrary function. The state variables as well as the evaporation and radiation fields are thus of the from:

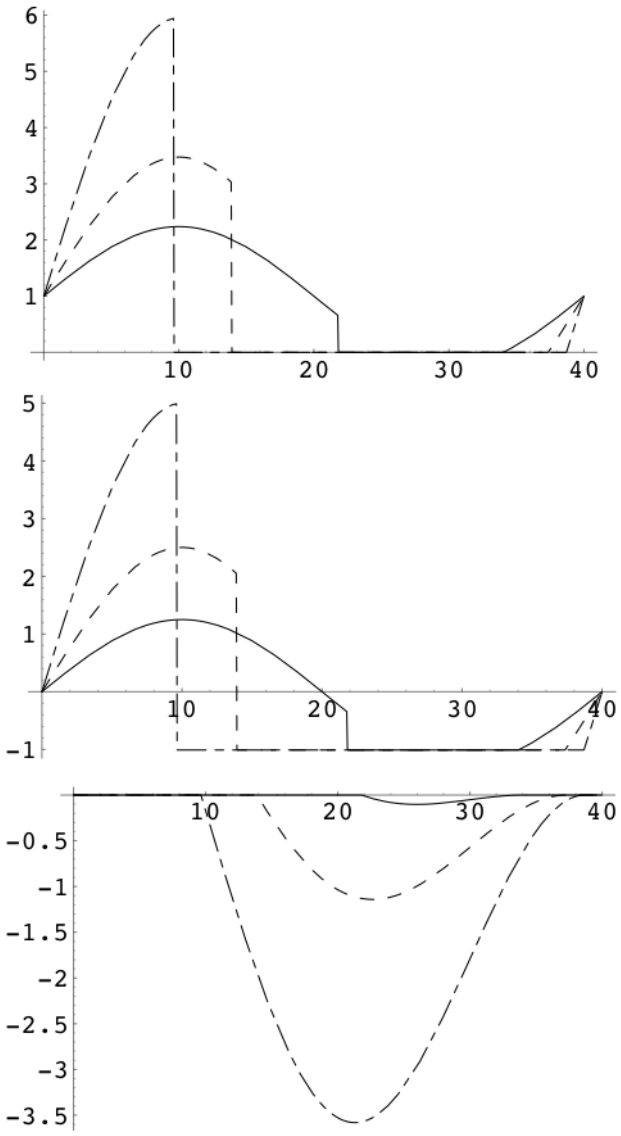

Figure 1. Solution for the one dimensional Walker circulation, for $\overline{\mathbf{U}} = -0.1c_d$, and $E_0 = 0.1$ (solid line), $E_0 = 0.2$ (dashed line) and $E_0 = 0.4$ (dash-dotted line). Upper panel: precipitation rate P. Middle panel: vertical velocity W. Lower panel: humidity Q.

$$u_1 = u_1(x)\exp(-\alpha y^2) \tag{40a}$$

$$v_1 = 0 \tag{40b}$$

$$T = T(x)\exp(-\alpha y^2) \tag{40c}$$

$$Q = Q(x)\exp(-\alpha y^2) \tag{40d}$$

$$R = R(x)\exp(-\alpha y^2) \tag{40e}$$

$$E = E(x)\exp(-\alpha y^2) \tag{40f}$$

The barotropic wind $\overline{U}$ is imposed, and assumed to be constant everywhere. We are looking for a solution of equations (39a-39d) in which the meridional velocity v vanishes. In this case, the zonal wind equation (39a) is the same as for the one-dimensional problem:

$$\overline{U}\partial_x u_1(x) = \partial_x T(x). \tag{41}$$

The meridional momentum budget (39b) becomes

$$\beta y u_1(x) = -2\alpha y T(x). \tag{42}$$

If the meridional structure of the solutions is such that

$$\alpha = -\frac{\beta}{2U}, \tag{43}$$

and if there exists an x_0 such that

$$T(x_0) = u_1(x_0) = 0, \tag{44}$$

then the equation for the zonal and meridional momentum (41) and (42) are equivalent. Equation (43) imposes the meridional structure of the special solution of the Walker cell, while (44) can always be met, as the temperature in this problem is defined up to an additive constant. Under these conditions, the equations are exactly the same as the one-dimensional Walker circulation equations, and the steady solutions to the one-dimensional problem can be extended to specific solutions of the two-dimensional Walker circulation. These special solutions are characterized by a purely zonal flow. For $-c_m < \overline{U} < 0$, these solutions can exhibit a stationary precipitation front at the Eastern edge of the moist region.

4. Riemann Problem

The three types of precipitation fronts found in section 2 each correspond to a different range of valid propagation speeds. These fronts move at a speed that is distinct from the dry or moist speed. Hence, such fronts intercept signals emanating from either the dry or moist regions. The expression (10) cannot be used directly to predict the propagation speed of a front. Indeed, the value of the vertical velocity on both side of the fronts depends in part of the behavior of the front itself. Instead, the front speed must be determined from the values of the Riemann invariants on the characteristics incident on the front.

4a. *Characteristics*

In the dry regions, the equations of motion (16a - 16c) can be rewritten as

$$\partial_t(W - \frac{T_x}{c_d}) - c_d\partial_x(W - \frac{T_x}{c_d}) = 0 \tag{45a}$$

$$\partial_t(W + \frac{T_x}{c_d}) + c_d\partial_x(W + \frac{T_x}{c_d}) = 0 \tag{45b}$$

$$\partial_t(\Delta\overline{Q}T_x + Q_x) = 0. \tag{45c}$$

These three equations describe the Riemann invariants

$$A_{dp} = W + \frac{T_x}{c_d} \tag{46a}$$

$$A_{dn} = W - \frac{T_x}{c_d} \tag{46b}$$

$$A_{dq} = \Delta\overline{Q}T_x + Q_x \tag{46c}$$

on three characteristics. The first two correspond to eastward and westward propagating gravity waves. The third is related to the quantity T_{w} introduced in section 2. It can be thought of as a moisture trace that retains information on the initial moisture distribution.

In the moist regions we have

$$\partial_t(W - \frac{T_x}{c_m}) - c_m\partial_x(W - \frac{T_x}{c_m}) = 0 \tag{47a}$$

$$\partial_t(W + \frac{T_x}{c_m}) + c_m\partial_x(W + \frac{T_x}{c_m}) = 0 \tag{47b}$$

$$Q_x = 0. \tag{47c}$$

These equations describe westward and eastward propagating waves moving at a speed c_m, with the corresponding invariants:

$$A_{mp} = W + \frac{T_x}{c_m} \tag{48a}$$

$$A_{mn} = W - \frac{T_x}{c_m}. \tag{48b}$$

Note that in SQE, only two Riemann invariants are sufficient to describe the flow in the moist regions.

The evolution of the flow for a given set of initial conditions can be determined by the method of characteristics. For an atmosphere that is uniformly dry or moist, it is straightforward to determine the flow at any time by using

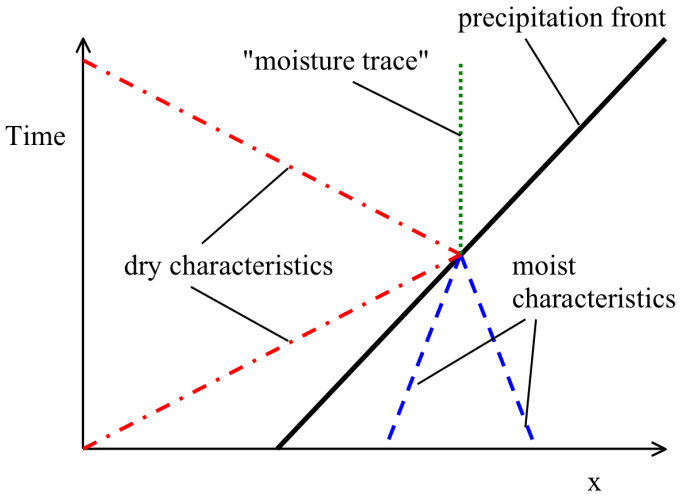

Figure 2. Schematic representation of the characteristics interacting with a propagating dry front. The front is propagating into the moist region, at a speed that is intermediate between that of the dry and moist characteristics. The moisture trace corresponds to the third characteristic in the dry region associated with the fluctuations of water vapor.

conservation of Riemann invariants along the different characteristics. In presence of a front, one must also determine the propagation speed and the value of the characteristics coming out of the front from the knowledge of the incident characteristics.

4b. *Drying front*

A dry front propagates into the moist region at a speed (relative to the ambient barotropic wind) between the dry and moist speeds, as illustrated in Figure 2. There are three incident characteristics: the two moist characteristics A_{mp} and A_{mn}, and the incident dry characteristic A_{dp} that catches up with the front from the dry side. From these, we need to determine the propagation speed of the front s, and the values of the two characteristics A_{dn} and A_{dm} that emanate from the front. This can be done by solving the system of equations (17a -17c), which yields:

$$s = \frac{2A_{dp} + (c_m - c_m^2)A_{mn} - (c_m + c_m^2)A_{mp}}{2A_{dp} - (1 - c_m)A_{mn} - (1 + c_m)A_{mp}} \tag{49a}$$

$$A_{dn} = \frac{A_{dp}A_{mp}(1 - c_m)^2 + A_{dp}A_{mn}(1 + c_m)^2 - 4A_{mp}A_{mn}c_m^2}{4A_{dp} - A_{mn}(1 - c_m)^2 - A_{mp}(1 + c_m)^2} \tag{49b}$$

$$A_{dq} = c_m(1 - c_m^2)\frac{(1 + c_m)A_{dp}A_{mn} - (1 - c_m)A_{dp}A_{mp} - 2c_mA_{mn}A_{mp}}{-2A_{dp} - (c_m - c_m^2)A_{mn} + (c_m + c_m^2)A_{mp}} \tag{49c}$$

The propagation speed s here is taken relative to the barotropic wind. It is a non-linear function of the incident characteristics. The upper panel of Figure 3 shows the variation of the front speed as a function of the incident dry

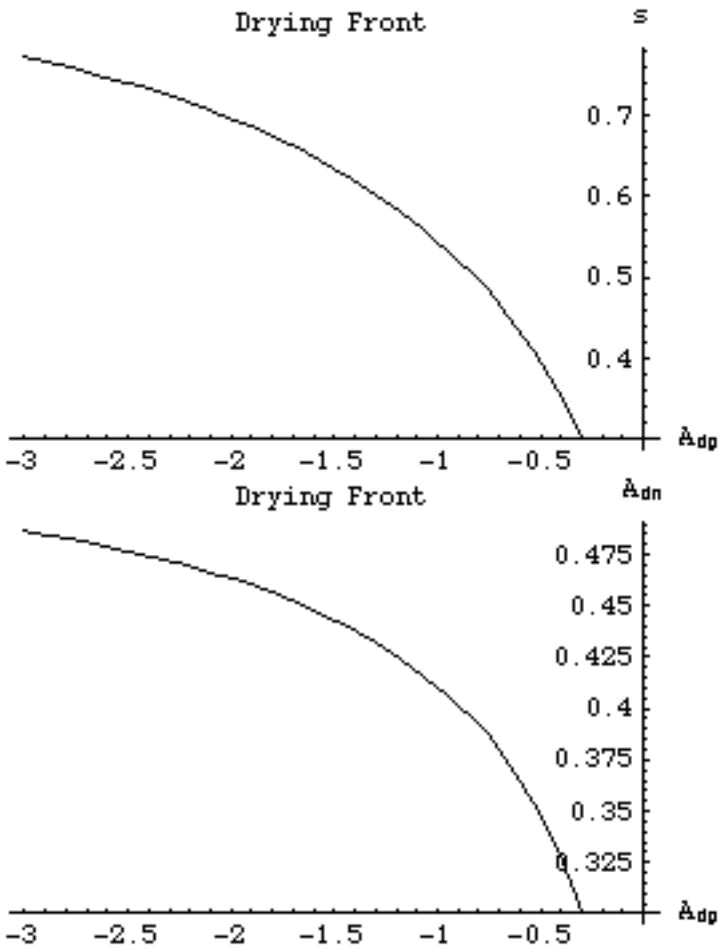

Figure 3. Upper panel: propagation speed of a dry front as a function of the amplitude of the incident dry wave, for $c_m = 0.3$, and $A_{mp} = A_{mn} = 1.0$. Lower panel: amplitude of the dry wave generated by a dry front as a function of the amplitude of the incident dry wave, for $c_m = 0.3$, and $A_{mp} = A_{mn} = 1.0$.

wave, for $c_d = 1$ and $A_{mp} = A_{mn} = 1.0$. For a weak incident dry wave with $A_{dp} \approx c_m A_{mn}$, the fronts move at a low speed, with $s \approx c_m$ to c_d. For a stronger dry incident wave with $A_{dp} >> A_{mn}$, the front speed becomes close to the dry propagation speed c_d. The lower panel of Figure **??** shows the amplitude of the dry gravity wave emanating from the same front.

4c. *Slow moistening front*

The slow moistening front propagates into the dry region at a speed between 0 and the moist speed, as illustrated in Figure 4. The slow moistening front intersects three characteristics: the dry and moist characteristics A_{dp} and A_{mn}, and the stationary moisture trace A_{dq}. The propagation speed s and the Riemann invariants on the two emanating

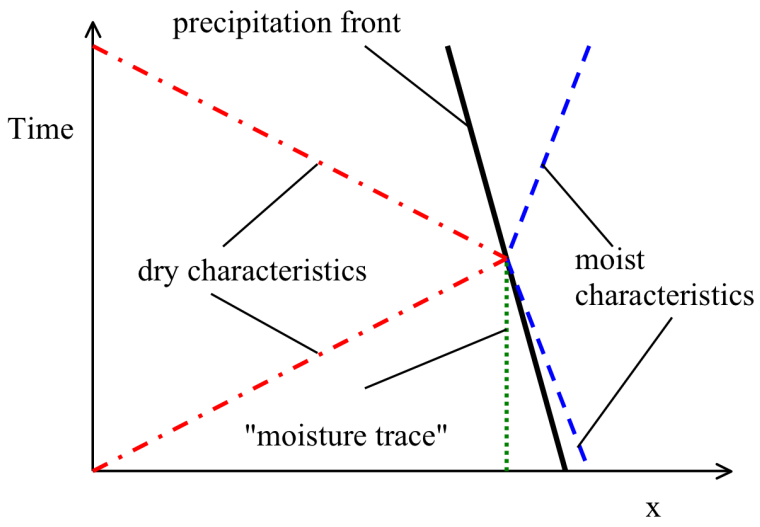

Figure 4. Same as Figure 2 but for the characteristics incident to a slow moist front propagating into the dry region at a speed lower than that of the moist characteristics.

characteristics A_{dn} and A_{mp} are obtained by solving (17a - 17c):

$$s = -\frac{(c_m - c_m^2)A_{dp} + c_m(c_m - c_m^2)A_{mn}}{A_{dq} - (c_m - c_m^2)A_{dp} + (c_m - c_m^2)A_{mn}} \tag{50a}$$

$$A_{dn} = \frac{-(1-c_m)c_m(1+c_m)^2 A_{dp}A_{mn} - (1-c_m)A_{dp}A_{dq} + 2c_m^2 A_{dq}A_{mn}}{(1+c_m)A_{dq} + c_m(1-c_m)(1-c_m^2)A_{mn} - 2c_m(1-c_m^2)A_{dp}} \tag{50b}$$

$$A_{mp} = \frac{A_{dp}A_{mn}(1-c_m)(1+c_m)^2 c_m + 2A_{dp}A_{dq} + A_{dq}A_{mn}(1-c_m)c_m}{c_m(1+c_m)(A_{dq} + A_{dp}(1-c_m)^2 + 2A_{mn}(1-c_m)c_m)} \tag{50c}$$

Figure 5 shows the propagation speed of a slow moistening front as function of the amplitude of the dry incident wave. When the incident dry and moist invariants are comparable with $A_{dp} \approx c_m A_{mn}$, the front speed is close to zero. The front speed increases to c_m as the ratio A_{mn}/A_{dp} increases.

4d. *Reflection and Transmission*

The precipitation fronts propagate at a speed that is distinct from that of the characteristics in moist and dry regions. The front speed is such that they always intercept three characteristics, while only two characteristics emanate from the front. When either side of the front is perturbed, a signal will propagate on a characteristic incident to the front. When the perturbation reaches the front, it will affect both the motion of the front and the characteristics emanating from it. While this is inherently a nonlinear problem, some insights can be gained by examining the linear version that arises when one considers the propagation of a small perturbation superimposed on a background flow.

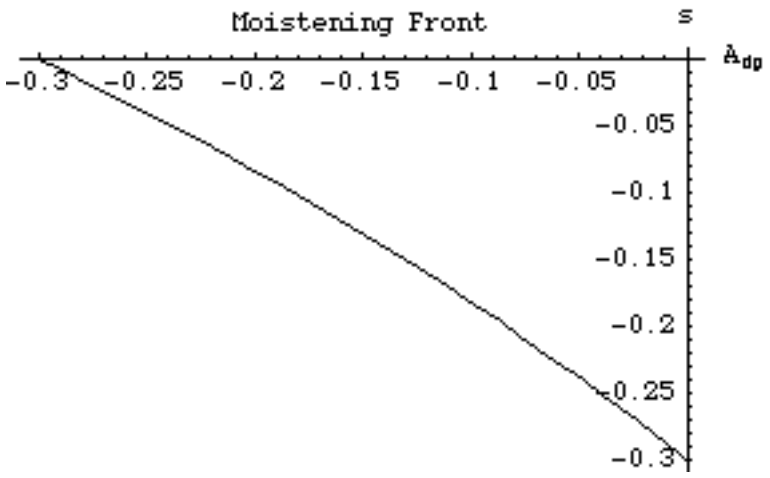

Figure 5. Propagation speed of a moist front as function of the amplitude of the incident dry wave, for $c_m = 0.3$, $A_{mn} = 1$, and $A_{dq} = 0$.

From a linear wave point of view, the moist and dry regions are characterized by two different refraction indices. The abrupt transition in the refraction index that occurs at the precipitation front results in partial refraction and partial transition of an incident wave. The reflection and transmission coefficients can be obtained directly by taking the partial derivative of equations (49b-49c), or (50b-50c). [§] For example the reflection coefficient for a incident dry wave on a dry front is given by

$$R = \frac{\partial A_{dn}}{\partial A_{dp}}|_{A_{mp},A_{mn}} \tag{51}$$

For any given front, we have a set of six different reflection-transmission coefficients given by the derivatives of the two outgoing amplitudes by the three incoming signals. These coefficient are not constant but depends on the incident characteristics. Figure 6 shows two of the reflection and transmission coefficients for a drying front as function of the magnitude of the incident dry characteristic A_{dp}. In addition, as the different characteristics have different speeds relative to the front, the frequency and wavelength of the reflected/transmitted signals will be different.

In addition to the two propagating gravity waves, the dry region has a third characteristic: the moisture trace A_{dq}. This characteristic accounts for the fluctuation of the water vapor content in the moist region, and interacts directly with the different front. As illustrated in Figures 2 and 4, a moisture trace emanates from a drying front, and intercepts a moistening front. In particular, when a moistening front encounters a perturbation in the water vapor content, gravity waves will be generated in both the dry and moist regions. For a small amplitude pertubation, Figure

[§] An alternative method for determining the reflection and transmission coefficients is to take advantage of the fact that the precipitation fronts are characterized by a discontinuity in the derivative of U, T, and Q, while the state variables remain continuous. This implies that the magnitude of the reflected and transmitted waves can be determined directly by imposing the continuity of U, T, and Q. This yelds a simple expression for the reflection and transmission coefficient expressed now in term of U, V, and T.

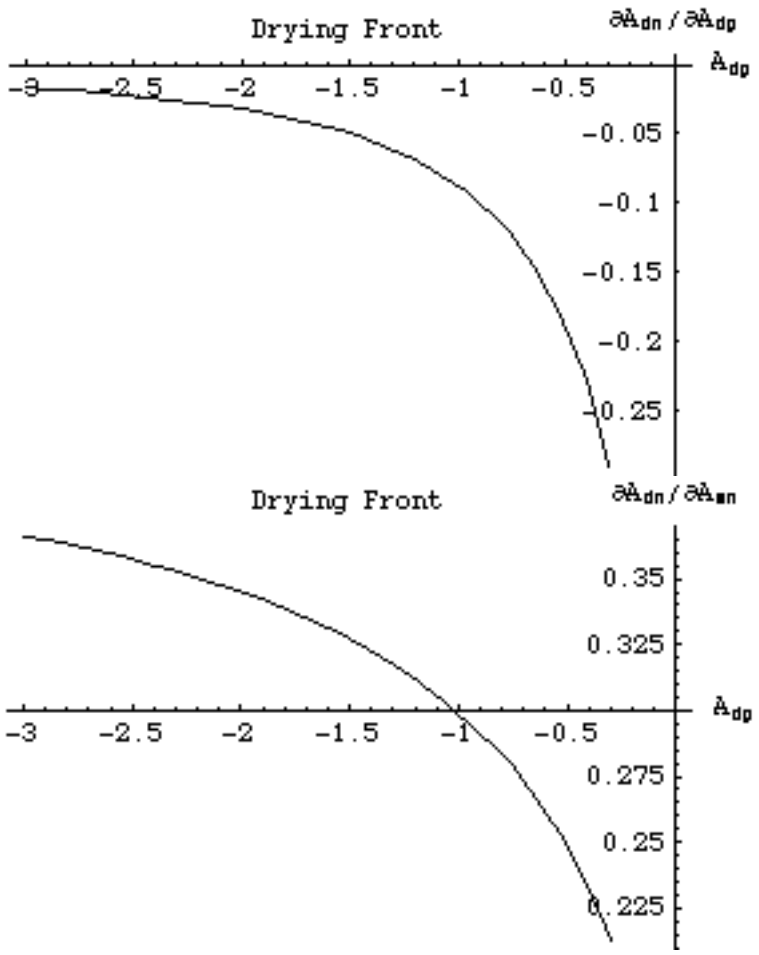

Figure 6. Reflection and transmission coefficients for a drying front as function of the incident dry wave , for $c_m = 0.3$, $A_{mn} = 1$, and $A_{mp} = 1$. Upper panel: reflection coefficient $\frac{\partial A_{dn}}{\partial A_{dp}}$ for an incident dry wave. Lower panel: Transmission coefficient $\frac{\partial A_{dn}}{\partial A_{mn}}$ for a moist wave moving toward the dry region.

7 show the 'reflection' and 'transmission' coefficients for a moisture trace perturbation incident on moistening front. 'Reflection' here refers to the gravity wave emanating in the dry region - the same side as the the moisture trace - while 'transmission' refers to the gravity wave propagating on the moist side - opposite to the moisture trace.

Remarkably, precipitation fronts allow for both over-reflection and

over-transmission of the incoming signal. Indeed, the upper panel of Figure 8 shows that the reflection coefficient for an incoming dry wave on a slow moist front can be larger than one. Similarly, The lower panel of Figure 8 indicates that the transmission coefficient for an incoming dry wave on the same slow moist front could be as large 5. In both cases, fluctuations in the vertical velocity are amplified after encountering the precipitation front. Such over-reflection and over-propagation should occur in both the freely propagating fronts and the stationary fronts discussed in section 3. This behavior has been observed in our numerical simulations (not shown). However, reproducing the exact magnitude of the theoretical value of the reflection coefficient did require the use short relaxation time of half an hour or shorter.

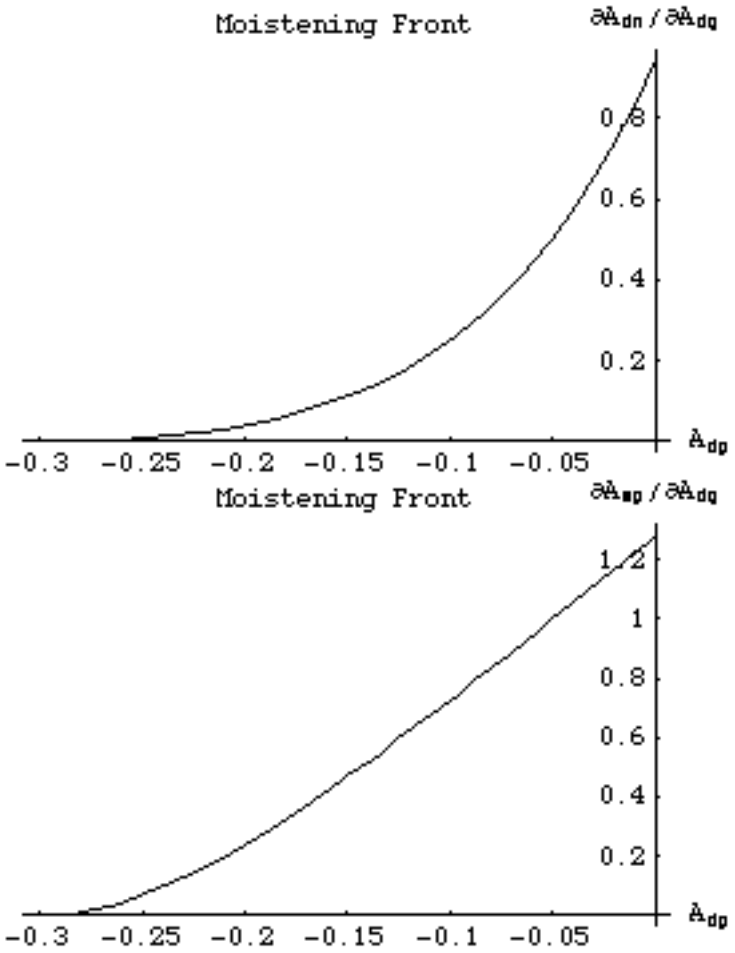

Figure 7. Reflection and transmission coefficient for the moisture trace incident to a moistening front for $c_m = 0.3$, $A_{mn} = 1$, and $A_{dq} = 0$, as function of the amplitude of the incident dry wave. Upper panel: 'reflection' coefficient $\frac{\partial A_{dn}}{\partial A_{dq}}$ for the gravity wave emanating in the dry region. Lower panel: 'transmission' coefficient $\frac{\partial A_{mp}}{\partial A_{dq}}$ for the gravity wave emanating in the moist region.

Longer relaxation time results in strong dissipation in the moist regions which tends to damp out the transmitted signal. While the results from the linear theory might indeed require very short relaxation time to be quantitatively accurate, they provide nevertheless a strong indication for amplification of disturbances after encountering a precipitation front – behavior that should be present even for larger, non-linear disturbances.

5. Discussion

We have shown that in the limit of very short relaxation time, the quasi-equilibrium assumption results in solutions with a discontinuity in the precipitation field and the first derivatives of the state variables. These discontinuities, called precipitation fronts, behave similarly to hydrodynamical shocks. Their propagation speeds can be obtained through a weak formulation of the equations of motions; these are distinct from the propagation speeds of the dry and moist

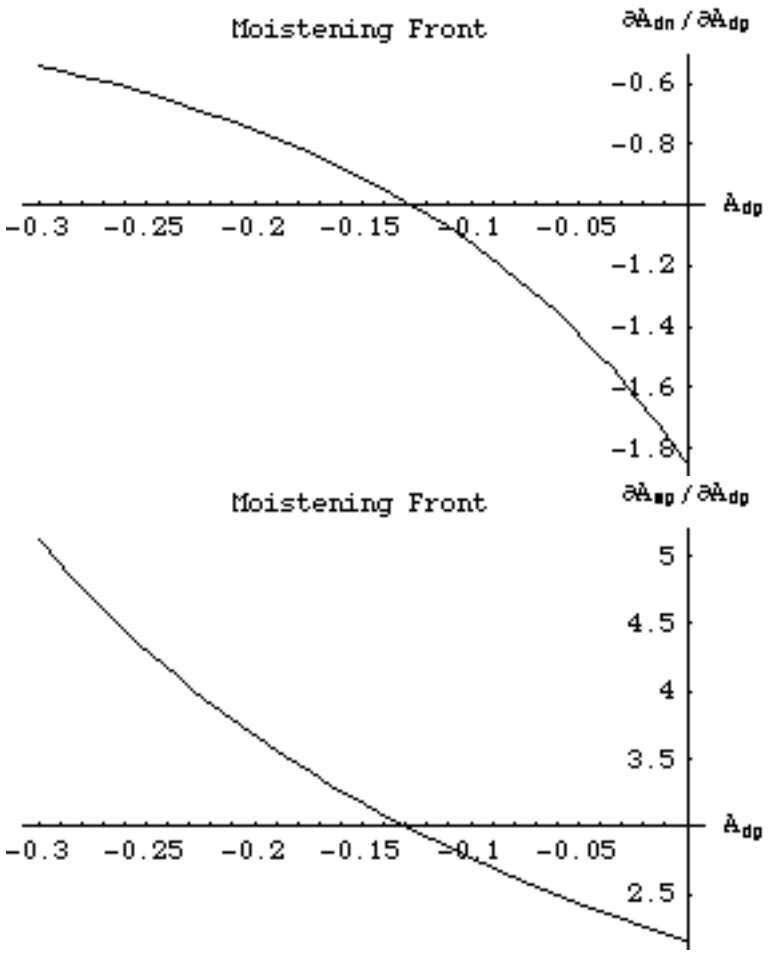

Figure 8. Reflection and transmission coefficient for a dry wave incident onto a moistening front for $c_m = 0.3$, $A_{mn} = 1$, and $A_{dq} = 0$, as function of the amplitude of the incident dry wave. Upper panel: Reflection coefficient $\frac{\partial A_{dn}}{\partial A_{dp}}$ for a moist front, as function of the amplitude of the incident dry wave, for $c_m = 0.3$, $A_{mn} = 1$, and $A_{dq} = 0$. Lower panel: transmission coefficient $\frac{\partial A_{mp}}{\partial A_{dp}}$ for a moist front, as a function of the amplitude of the incident dry wave, for $c_m = 0.3$, $A_{mn} = 1$, and $A_{dq} = 0$.

characteristics of the system. Only specific ranges for the values of the frontal speed are permitted, which allow one to classify the fronts into three categories: the drying front, the fast moistening front and the slow moistening front.

The theory for precipitation fronts outlined here, combined with the SQE framework of Emanuel et al. (1994), offers a very simple conceptual framework to discuss the dynamics of the tropical atmosphere. In this framework, disturbances in dry and moist regions obey the shallow water equations. The interfaces between dry and moist regions correspond to precipitation fronts. We have shown here how to obtain from the governing equations the propagation speed of the front as well as the values of the Riemann invariants emanating from the front. In this framework, the intrinsic nonlinearity associated with the requirement that precipitation is always positive is manifested in the nonlinear behavior of the precipitation fronts.

Disturbances encountering a precipitation front can be treated as moving between regions with different refractive

indices. Hence, perturbations incident to a precipitation front will partially reflect and partially propagate across the front. Reflection and propagation at the front are quite complex, and should be treated as a full non-linear problem. Nevertheless, a linear analysis confirms the reflection and refraction properties of the front, and indicates the possibility of over-reflection and propagation across the frontal boundary.

An intriguing extension of the one-dimensional theory discussed here is to investigate the propagation and reflection problem on an equatorial beta-plane. In this case, the linear solutions in the dry and moist regions would include Kelvin, Yanai and Rossby waves with the corresponding propagation speeds and Rossby radius. Solutions in the dry and moist regions would need to be matched at the interface between the dry and moist regions. The main difficulty lies in that the matching procedure must be performed along the entire interface, and not at a single location as was the case in the one dimensional problem. The two dimensional Walker solutions discussed here is one example of such a solution where a stationary front is conveniently located along a longitude line. As for the one-dimensional case, one does expect disturbances to partially propagate and transmit across the front. This implies for example that an incident Kelvin wave might be partially reflected as a Rossby wave when it moves from a moist to a dry region.

The mathematical framework for the precipitation fronts presented here is based on a simplified version of the QTCM for which it is possible to fully derive the dissipation of a moist available energy. In contrast to the full QTCM, this model omits the advection of the moisture by the baroclinic wind. Including such term adds a quadratic non-linearity and can induce new types of behavior. A particular concern is that large-scale convergence can steepen the moisture gradient and generate a discontinuity in finite time. While such behavior is a common consequence of advection and is unrelated to the convection, it makes it impossible to obtain a dissipation statement for the gradient formulation, as was done in section 2.c. The conditions that lead to an infinite increase in the humidity gradient are rather exceptional and not likely to corresponds to an actual circulation. Furthermore, the weak solutions for the precipitation fronts should still hold as long as there is no discontinuity in the state variables. Hence, while the detailed effects of a baroclinic moisture advection still need to be investigated, the existence and overall behavior of the precipitation fronts should not be affected.

Even though the precipitation front theory only describes the onset of precipitation in the limit of infinitely short adjustment time, it also offers a good approximation for solutions within finite convective adjustment time. Frierson et al. (2004) find that the propagation speed of precipitation fronts in SQE also serves to predict the speed at which the interface between dry and moist regions moves for finite values of the adjustment time. Khouider and Majda (2005) further confirm the existence of precipitation fronts in one and two dimensional numerical simulations. They also

provide examples of non-linear interactions between a precipitation front and an incident gravity wave. Stechmann and Majda (2006) show that for finite convective adjustment time, the frontal structure occupies a finite region, whose extent depends both on the frontal speed and the adjustment time. The frontal velocity and the far field difference between dry and moist regions are however well captured by the SQE preciptation front theory. Simulations also show that other theoretical predictions of the precipitation fronts, such as the location of stationary fronts, and the reflection/transmission of incident waves also occur with finite relaxation time.

The physical interpretation of precipitation fronts also sheds some light on the original quasi-equilibrium theory. In their original argument, Arakawa and Schubert (1974) argue that convection acts to balance destabilization by large-scale atmospheric motions. This adjustment is however not instantaneous, and one thus expects that convection will be unbalanced for a short period or small region. In the idealized model used, here, these adjustment regions are associated with the dissipation in the moist available potential energy (10) and its first derivative equivalent (14). The dissipative terms in these equations are associated with horizontal fluctuations of convective instability in the precipitation regions. In the limit of infinitely short adjustment time, the area where this dissipation occurs collapses onto the frontal singularity. For finite adjustment times however, there is a finite dissipative boundary layer at the interface between the dry and moist regions, as discussed in Stechmann and Majda (2006). This boundary layer corresponds to a zone where convective instability fluctuates, i.e., where convective adjustment cannot balance destabilization from external forcing. A key aspect of the precipitation front theory lies in that, while the boundary layer collapses in the limit of very short dissipation time, dissipation still takes place at the interface. In other words, right at the onset of precipitation, convection is unbalanced - even for infinitely short adjustment time. The finite extent of the precipitation fronts obtained by Stechmann and Majda (2006) corresponds to the region where convection has not yet equilibrated with the large-scale forcing, i.e. regions where significant convective instability would be present.

One may question whether precipitation fronts correspond to an actual phenomenon, rather than an interesting conceptual model. While this issue cannot be answered at this point, it should be stressed here that as precipitation fronts describe the onset of precipitation in the limit of instantaneous convective adjustment, they also offer a good approximation for the behavior of the interface between the dry and moist region for finite convective adjustment times. The precipitation fronts theory emphasizes the facts that the onset of precipitation introduces a very strong non-linearity in the system resulting in very complex behaviors. Given that many convection schemes used in General Circulation Models are based on quasi-equilibrium concepts, the mathematical description of the precipitation fronts presented here can serve as a prototype to explain the behavior of these more realistic models.

Acknowledgements

This work was supported by NSF grant ATM-0545047.

References

Arakawa, A. and W. H. Schubert, 1974: Interaction of a cumulus cloud ensemble with the large-scale environment, Part I. *J. Atmos. Sci.*, **31**, 674–701.

Betts, A. K., 1986: A new convective adjustment scheme. Part I: Observational and theoretical basis. *Quart. J. Roy. Meteor. Soc.*, **112**, 677–692.

Betts, A. K. and M. J. Miller, 1986: A new convective adjustment scheme. Part II: Single column tests using GATE wave, BOMEX, and arctic air-mass data sets. *Quart. J. Roy. Meteor. Soc.*, **112**, 693–709.

Bretherton, C., M. E. Peters, and L. E. Back, 2004: Relationships between water vapor path and precipition over the tropical oceans. *J. Climate*, **17**, 1517–1528.

Bretherton, C. S. and A. H. Sobel, 2002: A simple model of a convectively coupled Walker Circulation using the weak temperature gradient approximation. *J. Climate*, **15**, 2907–2920.

Emanuel, K. A., 1986: An air-sea interaction theory for tropical cyclones. Part I: Steady maintenance. *J. Atmos. Sci.*, **43**, 585–604.

— 1987: An air-sea interaction model of intraseasonal oscillations in the tropics. *J. Atmos. Sci.*, **44**, 2324–2340.

— 1991: A scheme for representing cumulus convection in large-scale models . *J. Atmos. Sci.*, **48**, 2313–2335.

Emanuel, K. A., J. D. Neelin, and C. S. Bretherton, 1994: On large-scale circulations in convecting atmospheres. *Quart. J. Roy. Meteor. Soc.*, **120**, 1111–1143.

Frierson, D. M. W., A. J. Majda, and O. Pauluis, 2004: Large scale dynamics of precipitation fronts in the tropical atmosphere: A novel relaxation limit. *J. Comm. Math. Sci.*, **2**, 591–626.

Khouider, B. and A. J. Majda, 2005: A non-oscillatory balanced scheme for an idealized tropical climate model. Part II: Nonlinear coupling and moisture effects. *Theoret. and Comp. Fluid Dyn.*, **19**, 355–375.

Lapeyre, G. and I. M. Held, 2004: The role of moisture in the dynamics and energetics of turbulent baroclinic eddies. *J. Atmos. Sci.*, **61**, 1693–1710.

Neelin, J. D., I. M. Held, and K. H. Cook, 1987: Evaporation-wind feedback and low-frequency variability in the tropical atmosphere. *J. Atmos. Sci.*, **44**, 2341–2348.

Neelin, J. D. and N. Zeng, 2000: A quasi-equilibrium tropical circulation model – formulation. *J. Atmos. Sci.*, **57**, 1741–1766.

Pauluis, O., 2004: Boundary layer dynamics and cross-equatorial Hadley circulation . *J. Atmos. Sci.*, **61**, 1161–1173.

Satoh, M., 1994: Hadley circulations in radiative-convective equilibrium in an axially symmetric atmosphere. *J. Atmos. Sci.*, **51**, 1947–1968.

Stechmann, S. N. and A. J. Majda, 2006: The structure of precipitation fronts for finite relaxation time . *Submitted to Theor. Comp. Fluid Dyn.*.

Wheeler, M. and G. N. Kiladis, 1999: Convectively coupled equatorial waves: Analysis of clouds and temperature in the wavenumber-frequency domain. *J. Atmos. Sci.*, **56**, 374–399.

Xu, K.-M. and K. A. Emanuel, 1989: Is the tropical atmosphere conditionally unstable? *Mon. Wea. Rev.*, **117**, 1471–1479.

Yu, J. Y., C. Chou, and J. D. Neelin, 1998: Estimating the gross moist stability of the tropical atmosphere. *J. Atmos. Sci.*, **55**, 1354–1372.

List of Figures